Analysis of Cell-seeded, Collagen-rich Hydrogel for Wound Healing

Daniel Sotelo Leon, MD*†
Tokoya Williams, MD*†
Zhen Wang, MD*†
Jacinta Leyden, MD*†
Austin Franklin, BA*†
Yukitoshi Kaizawa, MD, PhD*†
James Chang, MD*†
Paige M. Fox, MD, PhD*†

Background: Our laboratory has previously developed a novel collagen-rich hydrogel (cHG), which significantly increases the speed of wound healing in diabetic rats.
Methods: In this study, we examine the in vitro survival and migration of fibroblasts, endothelial cells, and adipose-derived stem cells in a novel cHG. Furthermore, we test the ability of adipose-derived stem cell–seeded cHG to support cell survival and accelerate healing in vivo.
Results: In vitro, cell survival within the cHG was retained for 25 days. We were unable to detect cellular migration into, out of, or through cHG. In the in vivo model, bioluminescence of stem cells seeded within the cHG in diabetic rat wounds was detected until day 10. Rate of wound closure was higher for cHG plus adipose-derived stem cells versus control from day 2 until day 16 and significant on days 6, 8, and 12 ($P < 0.05$). This significant difference was also observed on day 16 by histology ($P \leq 0.05$).
Conclusions: We conclude that cHG is a good candidate for delivering adipose-derived stem cells, endothelial cells, and fibroblasts to wounds. Future studies will determine whether the delivery of combinations of different cell lines in cHG further enhances wound healing. (*Plast Reconstr Surg Glob Open 2020;8:e3049; doi: 10.1097/GOX.0000000000003049; Published online 18 August 2020.*)

INTRODUCTION

Poor wound healing is associated with several factors, including tissue ischemia, local infection, and the presence of foreign bodies. This is further complicated by chronic diseases, such as diabetes and obesity, as well as other factors, including wound infection, advanced age, and stress.[1–3] Current wound care therapies include negative pressure wound therapy (NPWT), specialized wound dressings, and hyperbaric oxygen. Each of these treatment modalities attempts to address specific aspects of wound healing, like tissue ischemia or infection, but have limited prospective data about their efficacy[4] and clinical limitations. For example, NPWT, one of the current standards of care within the United States for chronic wounds, can be prohibitively expensive due to the machinery and dressings required.[5] Additionally, NPWT requires an airtight seal, which is difficult to achieve in deep or irregular wounds or near joints.[6] Other specialized treatments like Apligraf (Organogenesis, Canton, Mass.), a bilayer of fibroblasts (FBs) and keratinocytes derived from human foreskin, require application by health care providers, are sensitive to shearing forces, and have a limited application in deep ulcers due to their 2-dimensional shape.[7]

To address these challenges, we propose a novel human-derived collagen-rich hydrogel (cHG) that is able to provide both mechanical and molecular support for wound healing.[8] It is rich in type I collagen, a major component of normal skin.[9] The thermoresponsive nature of cHG allows it to conform to deep and irregular wounds while giving it a 3-dimensional framework for cellular support. The gelatinous nature of cHG prevents tissue edema and maintains the humidity necessary for wound healing.[10] Furthermore, cHG is easily applied with readily available equipment and is painless for the patient.

DOI: 10.1097/GOX.0000000000003049

This work was supported by
THE PLASTIC SURGERY FOUNDATION.

Because of its resemblance to human extracellular matrix, cHG may be able to promote the migration of endogenous cells into the wound[8] and act as a lattice that can be seeded with cells important for wound healing, such as FBs,[11] adipose-derived stem cells (ADSCs),[12] and endothelial cells (ECs).[13,14]

In this study, we investigate the ability of cHG to support the culture and migration of FBs, ADSCs, and ECs in vitro. Additionally, we use a stented-excisional wound model in diabetic rats to assess the ability of ADSC-seeded cHG to enhance wound healing in vivo.

MATERIALS AND METHODS

Preparation of cHG

cHG was synthesized using previously described methods.[8,15] Briefly, finger flexor tendons were harvested from fresh frozen cadaveric donors, decellularized, lyophilized, ground into a fine powder, and stored at –80°C. Samples were enzymatically digested in a 1 mg/mL solution of pepsin in hydrocloric acid to a final concentration of 25 mg/mL (2.5%) of tendon powder. Solution pH was adjusted to 2.2 for optimal pepsin digestion. After 14 hours, pepsin activity was reversed by increasing the pH of the solution to above 8 before adjusting the pH of the final solution to 7.4. The cHG was stored in liquid form at 4°C for up to 2 weeks.

Cell Seeding and Culture in Collagen Hydrogel

Commercially obtained ADSCs, FBs, and ECs (Cell Applications, San Diego, Calif.) were grown to confluence in a humidified tissue culture chamber using cell-specific growth media. At the time of seeding, cells were lifted from culture plates, placed in a suspension of fetal bovine serum (FBS; Lonza, Morristown, N.J.), and mixed into the 2.5% cHG solution. For ADSCs and FBs only, ×10 Minimum Essential Medium (Thermo Fisher Scientific, Waltham, Mass.) was added to the mix for nutritional support. The composition of the final solution was either (1) 80% cHG, 10% 10× Minimum Essential Medium, and 10% FBS (ADSCs and FBs) or (2) 80% cHG, 20% FBS (ECs), with the final concentration of tendon powder 20 mg/mL (2%). This mixture was incubated for 45 minutes at 37°C to allow for gelation. After addition of appropriate culture medium, seeded cHG was incubated in a humidified tissue culture chamber.

Cell Viability and Proliferation Assays

cHG was prepared to final concentrations of 2, 4, or 6 million cells per mL of seeded cHG. Ninety six–well plates were used with each well containing 100 μL samples of seeded cHG. After gelation, 200 μL of culture medium was added to each sample and replaced every other day. Samples were incubated for 0, 1, 5, 10, 15, 20, or 25 days. At each time point, samples were used for Live/Dead and proliferation assays.

To assess cell viability, we used Live/Dead Cell Viability/Cytotoxicity assay (Thermo Fisher Scientific). Live/Dead reagent was prepared according to the manufacturer's

instructions. After removal of cell culture medium, 100 μL of Live/Dead reagent was added to each sample. Samples were incubated at 37°C for 30 minutes and mounted onto a slide. The cells were visualized through fluorescence imaging and counted using Image J software (National Institutes of Health, Bethesda, Md.).

To assess cell proliferation, we used Quant-iT PicoGreen dsDNA assay (Thermo Fisher Scientific) for quantification of double stranded DNA at different time points. After incubation, cHG samples were harvested, frozen at –80°C, and lyophilized for 24 hours. Lyophilized samples were digested in papain at 60°C for 16 hours. Picogreen reagent was added to each sample, and DNA quantity was measured using a fluorescent plate reader. A known DNA standard curve was used to calculate the amount of DNA per gram of cHG in each sample. This was expressed as a multiple of the average amount of DNA on day 0 (proliferation coefficient).

We combined the results of the viability and proliferation assays into one graph by multiplying the average percent of viable cells by the mass of DNA per gram of cHG on each day. This was termed viable DNA mass. This allows us to estimate the amount of DNA present in viable cells, thereby creating an approximation of the viable and nonviable cellular mass present in the cHG at each time point.

In Vitro Migration Assays

Cell migration was assessed in 3 different ways: (1) migration through cHG (from cell-seeded cHG to nonseeded cHG) (Fig. 1); (2) migration from cell media into cHG; and (3) migration from cHG into cell media. Migration through cHG was measured by fluorescently labeling cells red using CellTracker Red CMTPX (Thermo Fisher Scientific) according to manufacturer's recommendations. Labeled cells were seeded into cHG at a concentration of 6 M/mL. A 3/8-inch cloning cylinder (Sigma-Aldrich, St. Louis, Mo.) coated with a thin layer of sterile silicone grease (Sigma-Aldrich) was placed in a 24-well plate to prevent migration of cells along the bottom of the dish. Hundred microliters of nonseeded cHG was placed inside the cloning cylinder, whereas 600 microliters of seeded cHG was placed outside of it. The
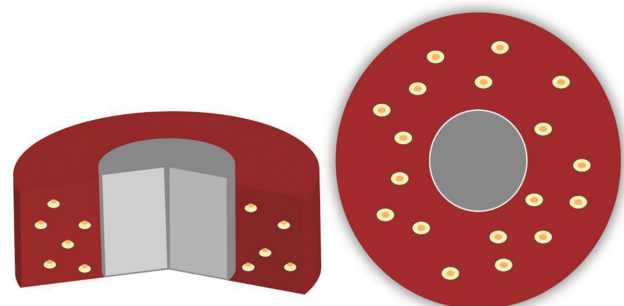
Fig. 1. A model of cHG cellular migration. Cells fluorescently labeled red (red region) are placed in a ring surrounding nonseeded cHG (gray region) in a 24-well plate. This construct is incubated for 7 days in a 24-well plate. Migration is tracked from the seeded into the nonseeded region. A, Sagittal cutaway. B, Top-down view.

cloning cylinder was removed, allowing contact between the seeded and nonseeded cHG regions. After gelation, the construct was incubated for 6 days, with fluorescent images taken every other day. Migration was tracked via Image J by counting the total number of fluorescently labeled cells in the seeded and nonseeded cHG regions.

Migration from cell media into cHG was measured by seeding fluorescently labeled cells into the appropriate cell media at a concentration of 0.5 million cells per milliliter. Nonseeded cHG was incubated in 96-well plates. For 6 days, 100 μL of seeded media was added to the surface of the nonseeded cHG, with the media replaced daily. After 6 days, the cHG samples were frozen and sectioned. The total number of cells present in cHG was quantified using fluorescent microscopy.

Migration from cHG into cell media was measured by preparing seeded cHG samples at the 6 M/mL concentration. Media was replaced every other day. Removed media was centrifuged. The supernatant was removed, replaced with Recovery cell culture freezing medium (Thermo Fisher Scientific), and stored at −80°C. After 6 days, frozen media was thawed and combined. The number of cells present in the thawed media was counted using a hemocytometer.

Stented-excisional Wound Model

This animal protocol was approved by our institutional review board. Eight male Zucker diabetic rats (16 weeks old; average weight, 400 g) were used (Envigo, Hayward, Calif.). Four 10-mm circular wounds were created on the dorsum of each rat following a previously established model.[15] The wounds were stented open using a 15-mm silicone ring and securely attached using sutures. Two wounds per rat were treated with occlusive dressing, and 2 wounds were treated with occlusive dressing plus 100 μL of cHG seeded with 2 M/mL ADSCs tagged with luciferase (Fig. 2), allowing each animal to serve as its own control group. Seeded cHG and occlusive dressing were reapplied every other day. Wound positions were alternated cranial/caudal and left/right on each rat to assure location on the dorsum did not affect healing. Differences in wound closure percentage were compared using *t* test analysis.

Cell survival in wounds was detected by applying luciferin mixed in 10 μL of ADSC media to all wounds and detecting bioluminescence using an in vivo imaging spectrum system (PerkinElmer, Waltham, Mass.). Wound closure was tracked using digital photographs taken every other day and analyzed using Image J. Animals were killed on day 16 for wound immunohistochemistry and histologic analysis.

Histology and Immunohistochemistry

Hematoxylin and eosin staining was used to examine wound architecture. Wound length, defined as the length of the gap between epithelial cells, was examined using Image J. Wound collagen content was assessed using Masson's trichrome stain. Immunohistochemistry was used to evaluate angiogenesis and cell proliferation using a mouse anti-rat EC antigen-1 (RECA-1) monoclonal antibody (MCA970R; Bio-Rad Laboratories, Hercules,
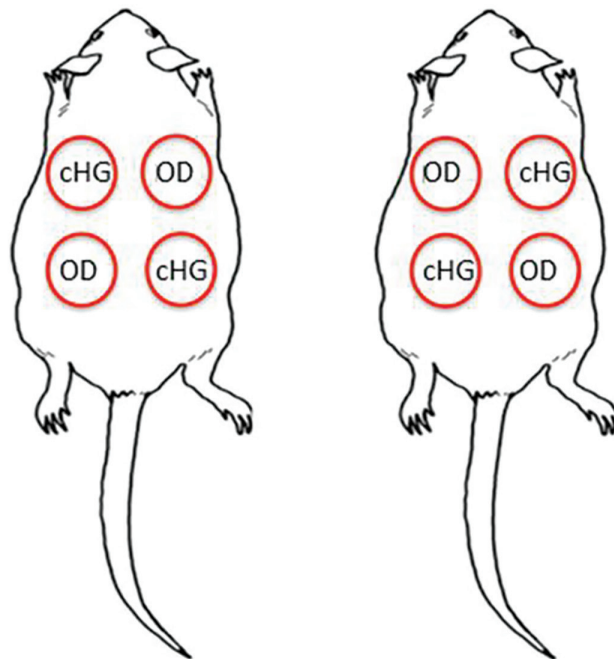
Fig. 2. The diagram showing configuration of wounds in the in vivo model. Wounds were alternated cranial/caudal and left/right to prevent wound location from affecting healing. cHG: Wounds receiving ADSC-seeded cHG plus occlusive dressing. OD: Wounds that received occlusive dressing only. OD indicates occlusive dressing.

Calif.) and a rabbit anti-rat antigen Ki67 polyclonal antibody (ab15580; Abcam, Cambridge, Mass.). RECA-1 is a cell surface antigen expressed by all rat ECs, and Ki67 is a nuclear protein present during cellular proliferation and absent during quiescent cellular stages.

Angiogenesis (RECA-1) and cell proliferation (Ki67) were quantified by computing the percentage of the area of the wound bed tagged by each antibody per high-power field image. Differences were examined using *t* test analysis.
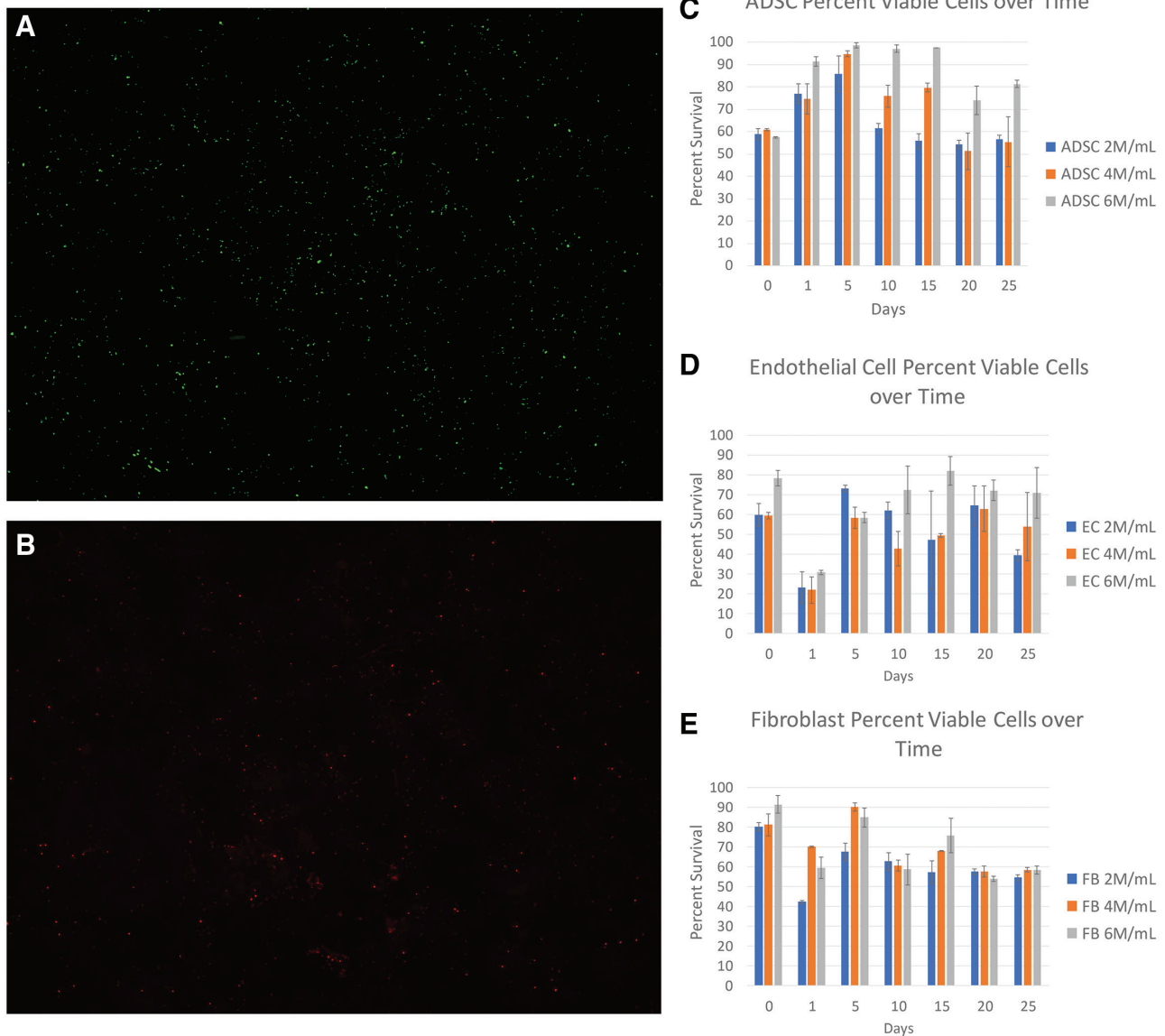
RESULTS

In Vitro Cell Viability and Proliferation Assays

The highest percentage of cell survival was seen at 6 M/mL concentration, with 58% (FBs), 71% (ECs), and 81% (ADSCs) of cells in each sample viable on day 25 (Fig. 3). This is compared with 58% (FBs), 54% (ECs), and 55% (ADSCs) for the 4 M/mL concentration and 54% (FBs), 39% (ECs), and 58% (ADSCs) for the 2 M/mL concentration. Through days 0–5, most of the seeded cells remained viable in the cHG, with most cell line concentrations having >55% viable cells on each of those days. Notable exceptions include the FB 2 M/mL concentration (42% viable cells) and ECs on day 1 (23%, 22%, and 31% for the 2, 4, and 6 M/mL concentrations, respectively).

Proliferation factor results are shown in Figure 4A–C. Overall, the quantity of DNA, which is correlated with the number of cells present in the sample, decreased on each consecutive day of the study. All cell concentrations had a similar rate of reduction in DNA quantity; however, as more cells are present initially in higher concentrations, there

Fig. 3. Results of Live/Dead assays showing the percentage of viable cells in cHG over time. A and B, Sample images showing microscopic images of viable (green) and nonviable (red) adipose-derived stem cells at ×10 magnification on day 0. C–E, Calculated percent viable cells over time for adipose-derived stem cells, endothelial cells, and fibroblasts.

was on average a higher amount of cell death in the higher concentrations compared with the lower concentrations. Each cell line and concentration combination approached an equilibrium concentration between 10% and 20% of the original cellular mass toward day 15. After this time point, the rate of DNA mass loss was much smaller.

Figure 4D–F shows viable DNA mass as defined above. The 6 M/mL concentration had a larger amount of viable cell mass than all other concentrations at any time point. This concentration also had a larger amount of nonviable cell mass than the other concentrations following day 1.

In Vitro Migration Assays

Migration through, into, and out of the gel was limited. The number of cells crossing into the nonseeded region after 6 days was in the hundreds. When examining migration from media into the gel, cells were not seen beyond the surface of the cHG after 6 days. Migration from cHG into media was quantified as a percentage of the total number of cells initially seeded into the cHG. After 6 days, 0.09% (FB), 0.14% (EC), and 0.11% (ADSC) of the initial cell load migrated from cHG into media.

In Vivo Stented-excisional Wound Model

There was a faster rate of wound closure in wounds treated with seeded cHG and occlusive dressing compared with those wounds treated with occlusive dressing only. This difference was statistically significant on days 6, 8, and 12 ($P < 0.05$) (Fig. 5). From day 6 to day 12, the average absolute wound closure percentage difference (wound
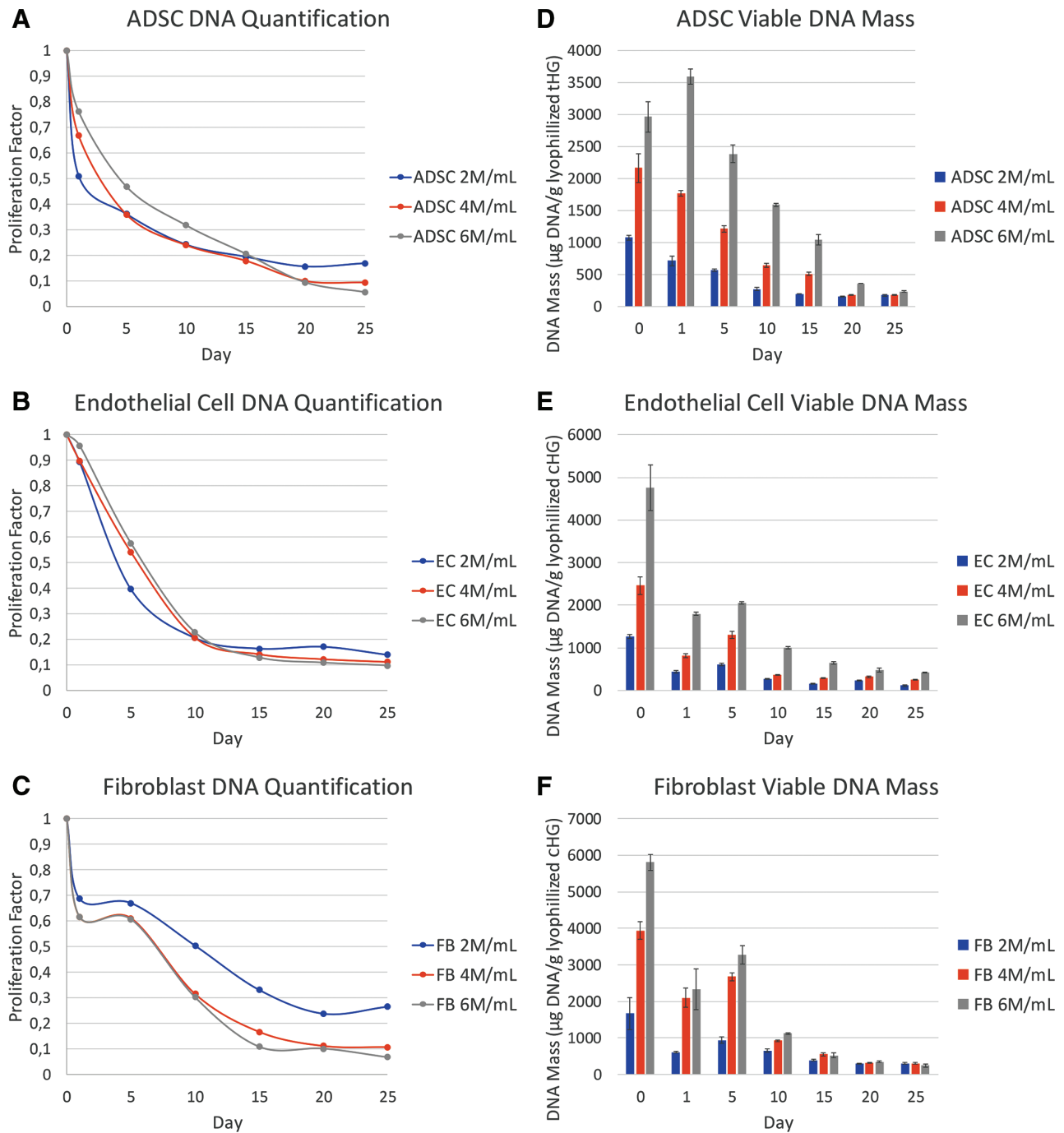
Fig. 4. DNA mass over time graphed as a factor of the DNA mass present on day 0 (proliferation factor, A–C) and viable DNA mass over time (mass of DNA present in live cells) (D–F). A and D, Adipose-derived stem cells. B and E, Endothelial cells. C and F, Fibroblasts.

closure percentage of seeded cHG-treated wounds minus that of the control wounds) ranged from 9.6% (day 8) to 12.2% (day 12). ADSC luciferase bioluminescence was detected in rat wounds through day 10.

Histology and Immunohistochemistry

On day 16, samples were obtained for histology and immunohistochemistry (Figs. 6–8). The average length of wounds treated with seeded cHG was significantly smaller

than control wounds (1444 and 2277 μm, respectively; $P < 0.05$). We observed a higher percent area of collagen in the seeded cHG treatment group compared with control (48.3% versus 35.5%; $P < 0.05$). RECA-1 staining revealed that angiogenesis was 4.9 times higher in the seeded cHG group compared with control ($P < 0.01$). Ki67 immunohistochemistry showed that cell proliferation in the seeded cHG group was 4.3 times higher than the control ($P < 0.05$).
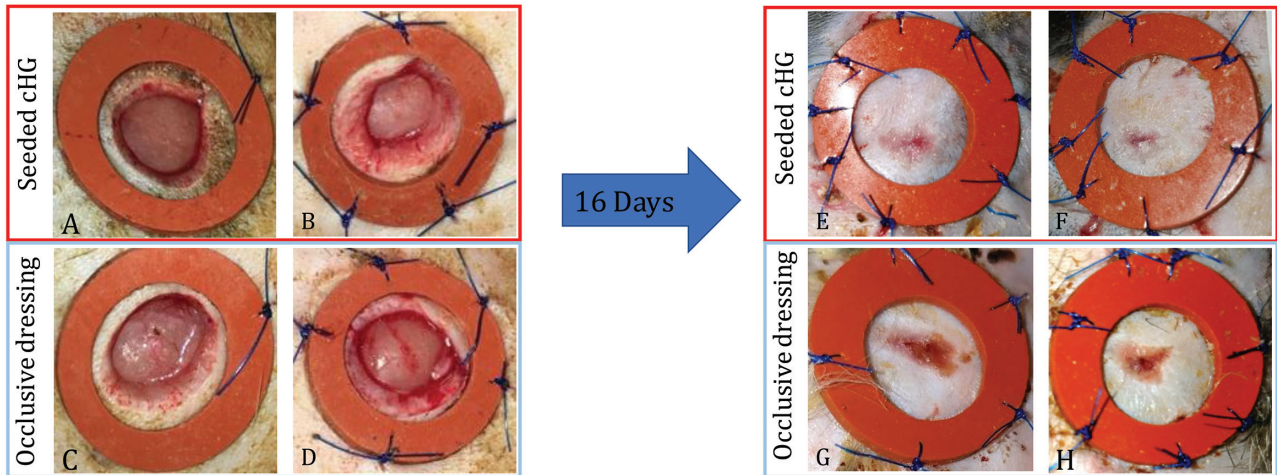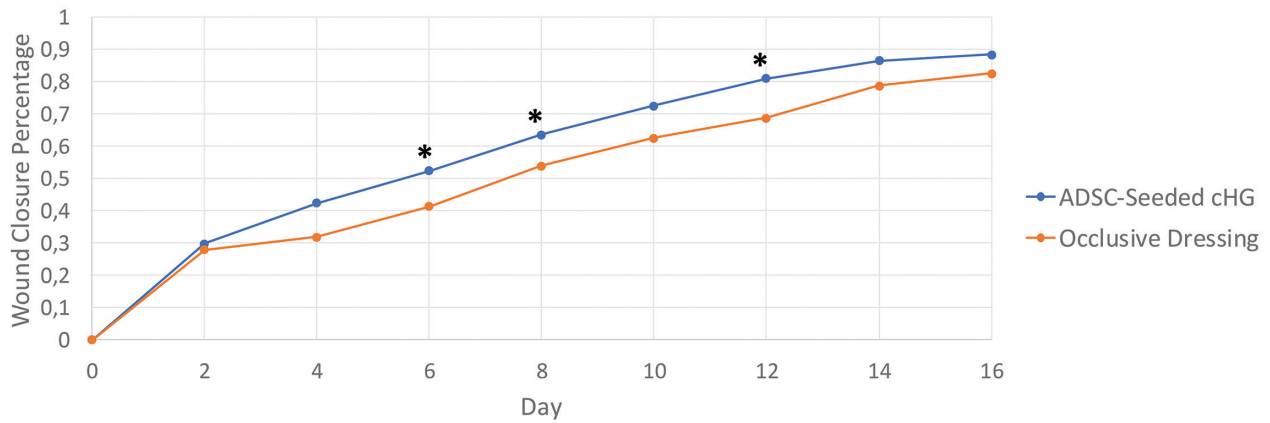
Fig. 5. Wound closure percentage data. A–H, Sample wound images after 16 days. The top row shows wounds treated with ADSC-seeded cHG and OD. The bottom row shows wounds treated with OD only. I, Average wound closure percentage over time. J, Bioluminescence signal of ADSC in cHG-treated wounds (right) compared with OD (left) detected on day 10. *Statistically significant difference in wound closure percentage, *P* < 0.05. OD indicates occlusive dressing.

DISCUSSION

We have previously studied the capacity of non-seeded cHG to enhance wound healing; the results of which have been previously published, which demonstrated that cHG independently enhances the speed of wound healing. Additionally, in preparing for this study, we investigated the possibility of topically applying cells without a carrier as a control group. Unfortunately, topical application of cells onto rat wounds leads to failure of cell survival as determined using in vivo bioluminescence imaging with labeled cells. The study presented here demonstrates the capacity of cHG to act as a carrier
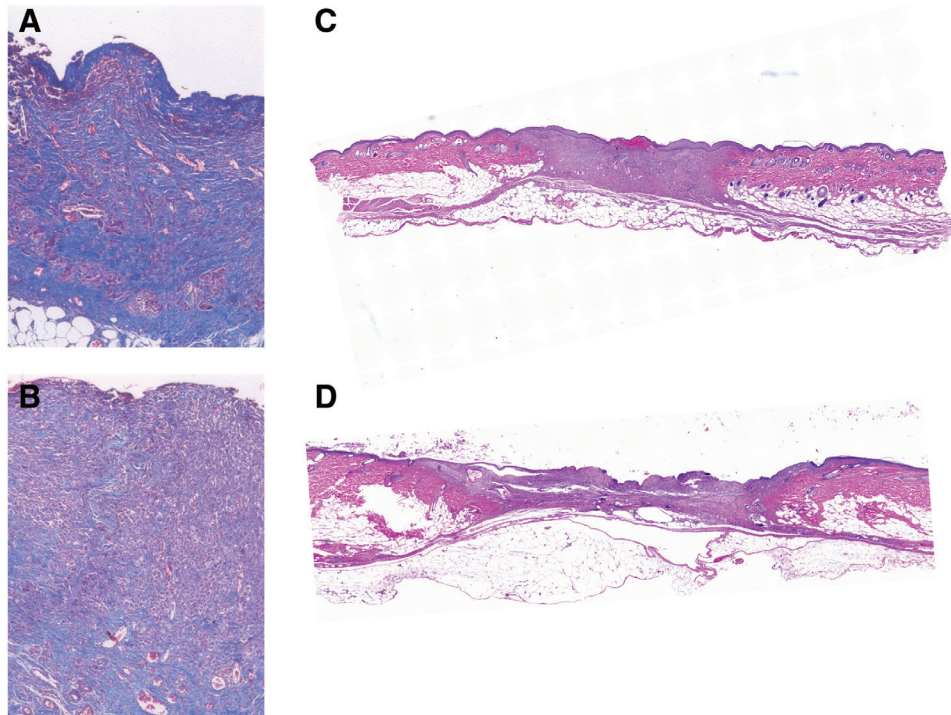
Fig. 6. Images showing day 16 histology. A and B, Trichrome stain. C and D, Hematoxylin and eosin stain. A and C, Wounds treated with seeded cHG plus OD. B and D, Wounds treated with OD only. OD indicates occlusive dressing.

of the aforementioned cell lines, which may be beneficial to enhance wound healing.

In vitro, cHG was able to support the survival of FBs, ECs, and ADSCs for 25 days. Across all cell lines, the 6 M/mL concentration had a greater proportion of viable cells present than the remaining concentrations. However, the 6 M/mL concentration also had large amounts of nonviable cells present. Achieving a balance in cellular augmentation of wound healing is important. Maximizing the number of viable cells delivered to the wound bed and minimizing the number of nonviable cells delivered to the wound bed help minimize excessive inflammation and pathologic tissue repair.[16–19] It is important to note that inflammation is an important part of the wound healing mechanism, and it is expected that both live and dead cells will cause a degree of inflammation in the wound bed. It is thus difficult to distinguish and quantify the inflammation that is caused by viable and nonviable cells.

We were unable to detect significant cellular migration through, into, or out of cHG in vitro. This may represent an inability of cells to navigate the cHG matrix. Alternatively, the absence of a chemotactic factor to drive cellular migration in vitro potentially limits cell migration. In vivo, this could mean that exogenous cells remain at the surface of the wound. However, the presence of chemotactic growth factor, such as platelet-derived growth factor, vascular endothelial growth factor, and FB growth factor, likely enhance the migration of not only the exogenous cells, but also promote the migration of endogenous stem cells to the wound in vivo.[20–23] We have used a rat model to examine the homing of systemic stem cells to

cHG and cHG +ADSCs, noting an increase in the attraction of endogenous cells to seeded cHG.[24]

In the in vivo model, ADSC-seeded cHG showed faster rates of wound closure compared with wounds treated with occlusive dressing only. This difference first became apparent on day 4 and became statistically significant on day 6 ($P < 0.05$). Previous studies in our laboratory have shown that cHG, when used on its own, is also able to accelerate wound healing.[16] However, there was no difference observed between nonseeded cHG and control until day 7, 3 days later than the effect seen with the cell-seeded cHG. Previous studies have shown ADSCs to be beneficial in enhancing endogenous wound healing, primarily through growth factor secretion.[12,17] Thus, by seeding the cHG, we may have enhanced the inherent wound healing properties of the cHG. Future studies will further elucidate this effect.

Furthermore, we showed that ADSCs can survive the transfer from cHG to the wound when seeded in cHG. ADSC luciferase bioluminescence was detected up to day 10 and absent from day 12 onward. It is possible that after day 10, the smaller wound diameter and depth lead to a lack of nutrition to adequately support the cells. Thus, after day 10, any benefit to wound healing is likely to arise from inherent cHG properties rather than from cellular augmentation. The addition of seeded cHG may be important in the early stages of healing, whereas, in later stages, nonseeded cHG is sufficient to provide accelerated wound healing.

Previous studies have shown the ability of ADSCs to enhance wound healing when seeded into hydrogels, with increased angiogenesis and proliferation compared
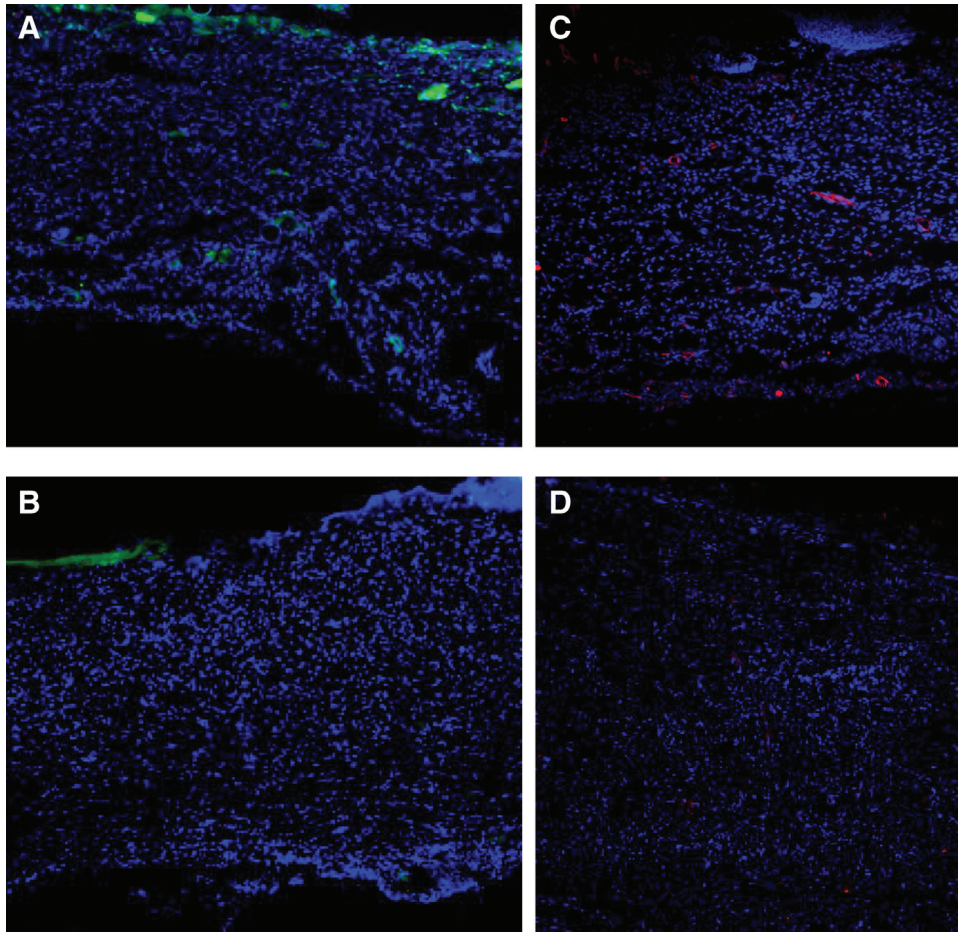
Fig. 7. Images showing day 16 IHC. A and B, Ki67 IHC (green) and DAPI stain (blue). C and D, RECA-1 IHC (red) and DAPI stain (blue). A and C, Wounds treated with seeded cHG plus OD. B and D, Wounds treated with OD only. IHC indicates immunohistochemistry; OD, occlusive dressing.
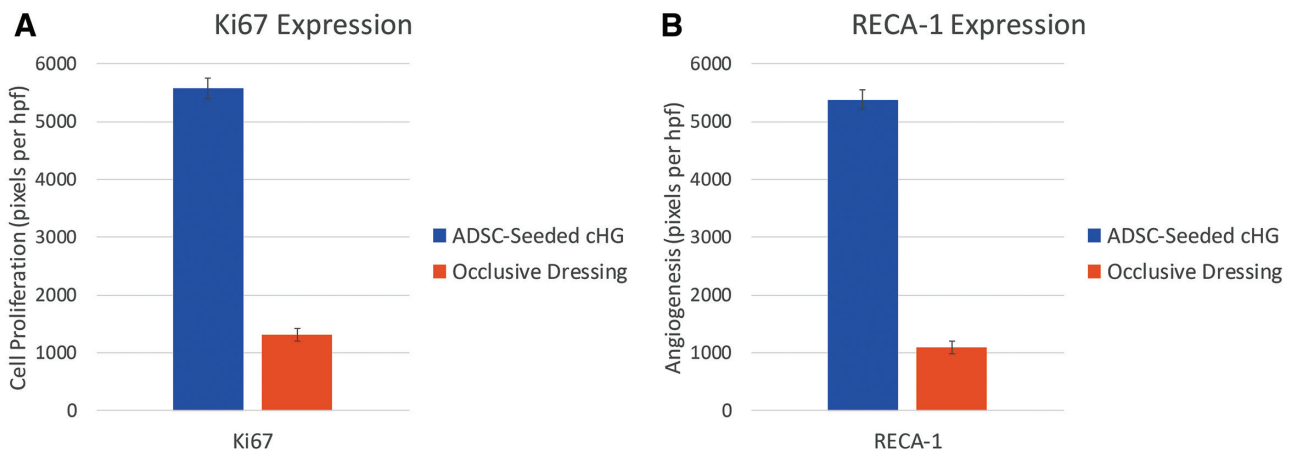
Fig. 8. Images showing day 16 IHC quantification. The area occupied by stained cells was quantified and expressed as number of pixels per high-power field. A, Ki67 expression. B, RECA-1 expression. Ki67 expression was 4.3 higher in seeded cHG-treated wounds compared with control. RECA-1 expression was 4.9 higher in seeded cHG-treated wounds compared with control. Hpf indicates high-power field; IHC, immunohistochemistry.

with nonseeded scaffolds.[18,19] Our histologic and immuno-histochemical analyses of cHG show similar results. cHG-treated wounds had significantly decreased wound length, increased collagen production, enhanced angiogenesis, and accelerated cell proliferation compared with control. These results further support cellular augmentation of cHG in improving the inherent wound healing benefit of cHG.

There are potential limitations to consider in this study. First, we used an in vitro model to study cell behavior within the hydrogel. This environment does not replicate the wound environment as it is missing chemokines, leukocytes, and growth factors present in the wound bed, as well as the cellular milieu, which may interact synergistically with cells present in the cHG. We hypothesize that cells delivered through cHG in vivo are likely to be more biochemically active, but further studies are needed. Finally, the calculated difference in wound closure percentage, although significant, was small. This is likely due to the small size of the initial wound (10 mm). In larger wounds, such as those seen in diabetic patients, the benefit from cHG may be greater due to its ability to enhance angiogenesis and cell proliferation, both of which are limited in this patient population.[25,26] Future studies will use larger initial wound sizes to more precisely determine long-term effects of seeded cHG application to wounds.

In summary, in this study, we have shown that cHG is able to support the survival of FBs, ECs, and ADSCs in vitro and that ADSC-seeded cHG is able to enhance wound healing in vivo in diabetic rats with improved angiogenesis despite limited migration in vitro. Further studies will examine the ability of chemotactic factors to induce cellular migration in cHG, as well as determine whether different cellular combinations can further enhance early stage wound healing with cHG.

Paige M. Fox, MD, PhD
Division of Plastic Surgery
Stanford University School of Medicine
770 Welch Road
Suite 400
Palo Alto, CA 94304
E-mail: pfox@stanford.edu

REFERENCES

1. Anderson K, Hamm RL. Factors that impair wound healing. *J Am Coll Clin Wound Spec*. 2012;4:84–91.
2. Guo S, DiPietro LA. Critical review in oral biology & medicine: factors affecting wound healing. *J Dent Res*. 2010;89:219–229.
3. Kalan LR, Brennan MB. The role of the microbiome in nonhealing diabetic wounds. *Ann N Y Acad Sci*. 2019;1435:79–92.
4. Frykberg RG, Banks J. Challenges in the treatment of chronic wounds. *Adv Wound Care (New Rochelle)*. 2015;4:560–582.
5. Kim JJ, Franczyk M, Gottlieb LJ, et al. Cost-effective alternative for negative-pressure wound therapy. *Plast Reconstr Surg Glob Open*. 2017;5:e1211.
6. Karadsheh M, Nelson J, Rechner B, et al. Application of a skin adhesive to maintain seal in negative pressure wound therapy: demonstration of a new technique. *Wounds*. 2017;29:E106–E110.
7. Zaulyanov L, Kirsner RS. A review of a bi-layered living cell treatment (Apligraf) in the treatment of venous leg ulcers and diabetic foot ulcers. *Clin Interv Aging*. 2007;2:93–98.
8. Farnebo S, Woon CY, Schmitt T, et al. Design and characterization of an injectable tendon hydrogel: a novel scaffold for guided tissue regeneration in the musculoskeletal system. *Tissue Eng Part A*. 2014;20:1550–1561.
9. Watt FM, Fujiwara H. Cell-extracellular matrix interactions in normal and diseased skin. *Cold Spring Harb Perspect Biol*. 2011;3:1–14.
10. Junker JP, Kamel RA, Caterson EJ, et al. Clinical impact upon wound healing and inflammation in moist, wet, and dry environments. *Adv Wound Care (New Rochelle)*. 2013;2:348–356.
11. Li B, Wang JH. Fibroblasts and myofibroblasts in wound healing: force generation and measurement. *J Tissue Viability*. 2011;20:108–120.
12. Kim WS, Park BS, Sung JH, et al. Wound healing effect of adipose-derived stem cells: a critical role of secretory factors on human dermal fibroblasts. *J Dermatol Sci*. 2007;48:15–24.
13. Johnson KE, Wilgus TA. Vascular endothelial growth factor and angiogenesis in the regulation of cutaneous wound repair. *Adv Wound Care (New Rochelle)*. 2014;3:647–661.
14. Bao P, Kodra A, Tomic-Canic M, et al. The role of vascular endothelial growth factor in wound healing. *J Surg Res*. 2009;153:347–358.
15. Chen JS, Longaker MT, Gurtner GC. Murine models of human wound healing. *Methods Mol Biol*. 2013;1037:265–274.
16. Williams T, Sotelo Leon D, Kaizawa Y, et al. Collagen-rich hydrogel augments wound healing in a diabetic animal model. *Ann Plast Surg*. 2020. [E-pub ahead of print].
17. Toyserkani NM, Christensen ML, Sheikh SP, et al. Adipose-derived stem cells: new treatment for wound healing? *Ann Plast Surg*. 2015;75:117–123.
18. Kosaraju R, Rennert RC, Maan ZN, et al. Adipose-derived stem cell-seeded hydrogels increase endogenous progenitor cell recruitment and neovascularization in wounds. *Tissue Eng Part A*. 2016;22:295–305.
19. Kaisang L, Siyu W, Lijun F, et al. Adipose-derived stem cells seeded in Pluronic F-127 hydrogel promotes diabetic wound healing. *J Surg Res*. 2017;217:63–74.
20. Schreier T, Degen E, Baschong W. Fibroblast migration and proliferation during in vitro wound healing. A quantitative comparison between various growth factors and a low molecular weight blood dialysate used in the clinic to normalize impaired wound healing. *Res Exp Med (Berl)*. 1993;193:195–205.
21. Yang M-H, Chang K-J, Zheng J-C, et al. Anti-angiogenic effect of arsenic trioxide in lung cancer via inhibition of endothelial cell migration, proliferation and tube formation. *Oncol Lett*. 2017;14:3103–3109.
22. Donovan J, Abraham D, Norman J. Platelet-derived growth factor signaling in mesenchymal cells. *Front Biosci (Landmark Ed.)* 2013;18:106–119.
23. Lamalice L, Le Boeuf F, Huot J. Endothelial cell migration during angiogenesis. *Circ Res*. 2007;100:782–794.
24. Franklin A, Min J, Oda H, et al. Homing of adipose derived stem cells to a tendon-derived hydrogel: a potential mechanism for improved tendon-bone interface and tendon healing. *J Hand Surg Am*. 2020. Jun 27:S0363-5023(20)30270-7
25. Cheng R, Ma JX. Angiogenesis in diabetes and obesity. *Rev Endocr Metab Disord*. 2015;16:67–75.
26. Brem H, Tomic-Canic M. Cellular and molecular basis of wound healing in diabetes. *J Clin Invest*. 2007;117:1219–1222.